Published in final edited form as:
Biochem J. 2012 August 15; 446(1): 47–58. doi:10.1042/BJ20120467.

Embryonic poly(A)-binding protein (EPAB) is required for oocyte maturation and female fertility in mice

Ozlem Guzeloglu-Kayisli[*], **Maria D. Lalioti**[*], **Fulya Aydiner**[*], **Isaac Sasson**[*], **Orkan Ilbay**[*], **Denny Sakkas**[*], **Katie M. Lowther**[†], **Lisa M. Mehlmann**[†], and **Emre Seli**[*,1]

[*]Department of Obstetrics, Gynecology and Reproductive Sciences, Yale University School of Medicine, 310 Cedar Street, LSOG 304D, New Haven, CT 06520, U.S.A

[†]Department of Cell Biology, UConn Health Center, 263 Farmington Ave, Farmington, CT 06030, U.S.A

Abstract

Gene expression during oocyte maturation and early embryogenesis up to zygotic genome activation requires translational activation of maternally-derived mRNAs. EPAB [embryonic poly(A)-binding protein] is the predominant poly(A)-binding protein during this period in *Xenopus*, mouse and human. In *Xenopus* oocytes, ePAB stabilizes maternal mRNAs and promotes their translation. To assess the role of EPAB in mammalian reproduction, we generated *Epab*-knockout mice. Although $Epab^{-/-}$ males and $Epab^{+/-}$ of both sexes were fertile, $Epab^{-/-}$ female mice were infertile, and could not generate embryos or mature oocytes *in vivo* or *in vitro*. $Epab^{-/-}$ oocytes failed to achieve translational activation of maternally-stored mRNAs upon stimulation of oocyte maturation, including *Ccnb1* (cyclin B1) and *Dazl* (deleted in azoospermia-like) mRNAs. Microinjection of *Epab* mRNA into $Epab^{-/-}$ germinal vesicle stage oocytes did not rescue maturation, suggesting that EPAB is also required for earlier stages of oogenesis. In addition, late antral follicles in the ovaries of $Epab^{-/-}$ mice exhibited impaired cumulus expansion, and a 8-fold decrease in ovulation, associated with a significant down-regulation of mRNAs encoding the EGF (epidermal growth factor)-like growth factors *Areg* (amphiregulin), *Ereg* (epiregulin) and *Btc* (betacellulin), and their downstream regulators, *Ptgs2* (prostaglandin synthase 2), *Has2* (hyaluronan synthase 2) and *Tnfaip6* (tumour necrosis factor α-induced protein 6). The findings from the present study indicate that EPAB is necessary for oogenesis, folliculogenesis and female fertility in mice.

Keywords

cytoplasmic polyadenylation; embryonic poly(A)-binding protein (EPAB); mouse; oocyte maturation; ovulation; translational activation

INTRODUCTION

In the mammalian ovary, oocytes arrested at the prophase of the first meiotic division reside within the ovarian follicles, where, depending on the stage of development, they are surrounded by one or more layers of granulosa cells (reviewed in [1]). Following female

[1]To whom correspondence should be addressed: emre.seli@yale.edu.

AUTHOR CONTRIBUTION

Ozlem Guzeloglu-Kayisli, Fulya Aydiner, Isaac Sasson, Denny Sakkas, Orkan Ilbay, Katie Lowther and Lisa Mehlmann generated the data. Ozlem Guzeloglu-Kayisli and Emre Seli were responsible for writing the paper. Maria Lalioti and Emre Seli directed the project.

sexual maturation, the pituitary gonadotropin FSH (follicle-stimulating hormone) promotes the cyclic growth of immature follicles to the pre-ovulatory stage (reviewed in [2]). This period of follicular growth is marked by proliferation of somatic cells, development of an antral cavity filled with follicular fluid, and oocyte growth and acquisition of competence to resume meiosis [3]. At the pre-ovulatory stage, the oocyte is surrounded by specialized granulosa cells called cumulus cells that are functionally distinct from the mural granulosa cells that line the antrum [4].

Following a surge in LH (luteinizing hormone), several critical steps are activated in the pre-ovulatory follicle: granulosa and cumulus cells are reprogrammed to express specific genes required for their terminal differentiation, cumulus cells produce an extracellular matrix, enabling them to move away from the oocyte, a process called cumulus expansion, and oocytes resume meiotic division and initiate maturation (reviewed in [5–7]). The collective result of these changes is the ovulation of a mature COC (cumulus–oocyte complex) containing an oocyte arrested at the metaphase of the second meiotic division (MII) and capable of being fertilized.

Oocyte maturation is associated with drastic changes in both the nuclear and cytoplasmic compartments, and with suppression of transcriptional activity (reviewed in [5]). Consequently, gene expression during oocyte maturation, fertilization and early embryo development, until ZGA (zygotic gene activation), is mainly regulated by timely translational activation of specific maternally-derived mRNAs, accumulated in the oocyte during the first meiotic arrest (reviewed in [8]). A primary pathway that mediates this process involves CPEB1 [CPE (cytoplasmic polyadenylation element)-binding protein 1], which promotes the cytoplasmic lengthening of poly(A) tails on mRNAs that contain an RNA motif called the CPE [9,10]. CPEB1 acts in concert with SYMPK (symplekin), CPSF (cytoplasmic polyadenylation specificity factor) and GLD2, an atypical poly(A) polymerase [9,11,12]. The regulation of translational activation during maturation is complex [13] and also involves at least one additional pathway, which involves DAZL (deleted in azoospermia-like) [14,15] and is independent of cytoplasmic polyadenylation.

The poly(A) tails of mRNAs are bound by a family of proteins called the PABPs [poly(A)-binding proteins], which promote translation and mRNA stability. In the oocyte, poly(A) tail length is a critical regulator of translation during maturation, and the oocyte contains a specific PABP, EPAB [embryonic poly(A)-binding protein] [16]. Initially identified in *Xenopus laevis* [16], EPAB is conserved in mammals [17–19] and differs from somatic PABP (PABPC1), primarily in the region between its conserved RRMs (RNA-recognition motifs) and the PABC (C-terminal) domain. In *Xenopus* oocytes, ePAB interacts with the CPEB1–SYMPK–CPSF [20] and DAZL–Pumilio [14] complexes, prevents deadenylation of mRNAs [16], enhances translation initiation [18] and promotes cytoplasmic polyadenylation *in vitro* [20]. We have recently reported that, in *Xenopus* oocytes, EPAB is a dynamically modified phosphoprotein and showed that EPAB phosphorylation at a four-residue cluster is required for cytoplasmic polyadenylation and oocyte maturation [21].

In the mouse, *Epab* mRNA is exclusively expressed in germ cells and one- and two-cell embryos [17,22], and is replaced by *Pabpc1* upon ZGA [17], which occurs at the two-cell stage [23]. Given its tightly controlled expression at a time when transcription is suppressed, we hypothesized that EPAB may play a key role in the regulation of gene expression during early mouse development and generated *Epab*-deficient mice by targeted deletion of the *Epab* gene. We found that EPAB is required for cytoplasmic polyadenylation and oocyte maturation in the mouse. In addition, EPAB's absence results in suppression of cumulus expansion and ovulation. Overall, our findings demonstrate that EPAB is a central regulator of oogenesis and folliculogenesis and is required for female fertility.

MATERIAL AND METHODS

Generation of *Epab* knockout mice

Mice were bred and maintained according to the Yale University animal research requirements, and all procedures were approved by the Institutional Animal Care and Use Committe (protocol number 2011-11207). The Epab-targeting construct was prepared in the pEasyFlox vector (provided by Manolis Pasparakis, Institute for Genetics of the University of Koeln, Cologne, Germany) [24,25]. An upstream 5.2 kb ClaI/BamHI fragment and a 2.5 kb downstream SalI/XhoI fragment were amplified from mouse genomic DNA using Pfu polymerase (Stratagene), cloned in pCRII-TOPO (Invitrogen), sequenced, and subcloned into pEasyFlox as arms for homology (Figure 1A). ESCs (embryonic stem cells) from 129Sv/C57BL/6 hybrid mice were transfected and selected at Yale University Animal Genomic Services (New Haven, CT, U.S.A.). $Epab^{+/-}$ ESCs were injected into C57BL/6 blastocysts to produce chimaeras. Mating male chimaeras with C57BL/6 females produced heterozygous offspring. The *Neo* gene was removed by crossing heterozygous mice with the CMV-*Cre* transgenic mice. Breeding of heterozygous mice produced homozygous *Epab*-deficient mice ($Epab^{-/-}$) with a Mendelian distribution. Homologous recombination was confirmed using Southern blot analysis and genomic PCR. Production of only targeted transcripts in $Epab^{-/-}$ mice was demonstrated using RT (reverse transcription)–PCR. The primers used for genomic PCR and RT–PCR are shown in Supplementary Table S1 (at http://www.BiochemJ.org/bj/446/bj4460047add.htm).

Assessment of fertility

To evaluate the fertility of $Epab^{+/+}$, $Epab^{+/-}$ and $Epab^{-/-}$ female mice, nine female mice from each group (4–5-week-old) were mated with adult (12-week-old) WT (wild-type) males of proven fertility for 20 weeks. Two female mice were housed with one 12-week-old male mouse, and male mice were rotated weekly. Cages were monitored daily, and the number of litters and pups were recorded. The fertility of $Epab^{-/-}$ male mice was similarly assessed.

Histomorphometric analysis of folliculogenesis in ovaries

Ovaries were fixed in Bouin's solution (Sigma–Aldrich) overnight, dehydrated in ethanol and embedded in paraffin. Serial sections (5 μm thick) of paraffin-embedded ovarian tissues were stained with haematoxylin and eosin or Periodic acid–Schiff stain using a standard protocol [26]. Every fifth section was assessed, and the total number of follicles for each ovary was determined by counting the follicles containing oocytes with a visible nucleus. Primordial, primary, secondary, early antral and antral follicles were classified as described previously [27]. Briefly, primordial follicles were defined as an oocyte surrounded by a layer of squamous granulosa cells. Primary follicles possessed an oocyte surrounded by a single layer of cuboidal granulosa cells. Secondary follicles were surrounded by two or three layers of cuboidal granulosa cells with no visible antrum. Early antral follicles were surrounded by four or more layers of granulosa cells, forming the follicular antrum. Antral follicles contained a clearly defined single antral space.

Assessment of the oestrous cycle

Vaginal smears from WT and $Epab^{-/-}$ female mice at 12 weeks old were assessed daily between 10:00 h and 12:00 h using a pipette tip and sterile PBS. The smear was classified into one of four phases of oestrous: elongated nucleated epithelium indicated pro-oestrous; large cornified epithelial cells were found in oestrous; metoestrous was marked by a thick smear composed of equal numbers of nucleated epithelial cells and leukocytes; and a smear consisting almost exclusively of leukocytes depicted dioestrus [28]. Cycle length for each

animal was determined by assessing the length of time between two oestrous cycles for a period of at least four consecutive cycles. The length of the oestrous cycle and the number of days spent at each stage of the cycle were determined for each animal.

Oocyte and embryo collection

Mouse oocytes and two-cell embryos were collected using standard protocols [17]. Briefly, mature female mice were superovulated by intraperitoneal injection of 5 IU of PMSG (pregnant mare serum gonadotropin) (Folligon, Sigma–Aldrich) to stimulate follicle development. To collect oocytes arrested at PI (prophase I) or GV (germinal vesicle) stage, mice were killed 44 h later by CO_2 inhalation, the ovaries removed, and oocytes were isolated by puncturing the ovaries with a 26-1/2 G needle under the dissecting microscope (Olympus SZH-ILLK). To obtain mature oocytes or embryos, an additional injection of 5 IU of hCG (human chorionic gonadotrophin) (Chorulon, Sigma–Aldrich) to induce oocyte maturation and ovulation was given 48 h after the PMSG injection. Unfertilized oocytes at metaphase of the second meiotic division (MII) were collected from oviducts 14 h after the hCG injection. To obtain fertilized embryos, females were placed individually with 12-week-old WT males immediately after the hCG injection. The following morning, the effectiveness of mating was confirmed by the presence of a vaginal plug (day 1). Two-cell embryos were collected 42 h after hCG injection from the oviducts into Hepes-buffered HTF (human tubal fluid) medium (Irvine Scientific). Removal of the cumulus cells was achieved in Hepes-buffered medium containing 1 mg/ml hyaluronidase (Sigma–Aldrich).

In vitro oocyte maturation

GV-stage oocytes were collected into Liebovitz's L-15 medium (Invitrogen) containing 5 % (v/v) FBS (fetal bovine serum; Invitrogen), 100 units/ml penicillin, 100 μg/ml streptomycin (Invitrogen) and IBMX (isobutylmethylxanthine) (250 μM), to prevent GVBD (GV breakdown). For *in vitro* maturation, denuded GV oocytes were washed in Liebovitz's L-15 medium without IBMX and incubated in α-MEM (minimal essential medium)-Glutamax (Gibco Invitrogen) with 5 % (v/v) heat-inactivated FBS, 5 μg/ml insulin, 10 μg/ml transferrin, 5 ng/ml selenium (ITS; Gibco-Invitrogen) and 100 mIU/ml recombinant FSH (Puregon, Organon). Oocytes were assessed for GVBD (consistent with metaphase I stage), and appearance of a polar body (consistent with MII stage) every 2 h for a period of 18 h. The percentage of GVBD and MII oocytes were recorded and averaged at each time point.

Immunostaining of oocytes

Oocytes at different stages of *in vitro* maturation were fixed in 4 % (w/v) paraformaldehyde in PBS (pH 7.4) for 30 min, permeabilized in 0.5 % Triton X-100 for 20 min, and blocked in 1 % (w/v) BSA for 1 h. Then, oocytes were incubated with anti-α-tubulin–FITC antibody (1:50, Sigma F-2168, clone DM1A) for 1 h, washed three times for 5 min in PBS with 0.1 % Tween 20 and 0.01 %Triton X-100, and stained with DAPI (4′,6-diamidino-2-phenylindole) prior to being assessed under a fluorescent microscope (Carl Zeiss Axioplan 2 with an AxioCam HRC camera system). All steps were performed at room temperature (22 °C).

PCR based-poly(A) tail assay

Lengths of mRNA poly(A) tails were determined using a PCR-based poly(A) tail assay as described previously [29]. Briefly, total RNA was isolated using an RNAqueous Microkit (Ambion) from 100 oocytes, treated with DNase, and RNA was ligated to phosphorylated oligo$(dT)_{12–18}$. Then, RT was carried out using Super Script II (Invitrogen) and an oligo-anchor primer. Subsequently, PCR was performed using a gene-specific upstream primer against the gene of interest and a reverse primer against the anchor. The minimum expected sizes of amplified products were: 152 bp for *c-Mos* [122 bp *c-Mos* 3′-end plus 30 bp

oligo(dT)-anchor], 100 bp for *Ccnb1* (cyclin B1) [72 bp of *Ccnb1* 3′-end plus 30 bp oligo(dT)-anchor], 114 bp for *Dazl* [84 bp *Dazl* 3′-end plus 30 bp oligo(dT)-anchor], and 200 bp for *Actb* (*β*-actin) [170 bp *Actb* 3′-end plus 30 bp oligo(dT)-anchor]. PCR products were electrophoresed on a 2.5 % agarose gel stained with 0.5 mg/ml ethidium bromide.

Preparation and microinjection of *Epab* mRNA

The mouse full-length *Epab* was amplified from the pCR4-m*Epab* vector (GenBank code BC158030; IMAGE code 9007333; Open Biosystems) and a HA (haemagglutinin) tag was fused in-frame at the 3′-end using PCR with forward primer Epab.C-F (5′-GGGACTAGTCATCATGGACACAGGTGGCCATGGC-3′) and reverse primer Epab.C-R (5′-CCCCTCGAGTTAAGCGTAATC-TGGAACATCGTATGGGTATTCGAAGTTCCTATCTGTTGA-CTCCATTTC-3′). The PCR product was cloned into the pCR2.1 vector using a TOPO-TA Cloning Kit (Invitrogen). Insert direction and sequence were confirmed by sequencing with M13F and R primers.

pCR2.1-mEpab-HA vector was linearized with HindIII and used as a template for *in vitro* transcription using mMESSAGE mMACHINE® T7 Kit (Ambion). Following *in vitro* transcription, mRNAs were polyadenylated using a Poly(A) Tailing Kit (Ambion), purified using an RNeasy Mini Kit (Qiagen), and stored at −80 °C in nuclease-free water until microinjection.

Microinjections were performed as described previously [27,30]. Briefly, fully grown GV-stage oocytes from WT and *Epab*$^{-/-}$ mice were quantitatively microinjected with ~3 pg *Epab* mRNA (in 10 pl total volume), and then incubated overnight in culture medium supplemented with 10 μM milrinone to maintain meiotic arrest. The next day, oocytes were washed to remove the milrinone and cultured for *in vitro* maturation in culture medium.

Western blot analysis

Oocyte lysates (100 oocytes per sample, except for microinjected oocytes, where 10 oocytes per sample were used) prepared in M-PER mammalian protein extraction reagent (Thermo Scientific), supplemented with protease inhibitory cocktail (Calbiochem), were separated by SDS/PAGE [10 % Tris-HCl Ready gels (Bio-Rad Laboratories)] and transferred on to nitrocellulose membranes. Membranes were blocked with 10 % (w/v) non-fat dried skimmed milk powder in TBS-T [TBS (20 mM Tris/HCl and 150 mM NaCl) plus 0.05 % Tween 20 at pH 7.4] for 1 h at room temperature and incubated with primary antibodies [1:500 dilution in 5 % (w/v) non-fat dried skimmed milk powder in TBS-T] overnight at 4 °C. After washing in TBS-T, membranes were incubated with horseradish peroxidase-conjugated anti-rabbit secondary antibody (1:2000; Vector Laboratories) for 1 h at room temperature. Signals were detected using ECL Plus reagent (Amersham Life Sciences). Antibodies against cyclin B1 and *β*-actin were from Cell Signaling, antibodies against DAZL and CPEB1 were from Abcam, and anti-HA antibody was from Roche.

qRT-PCR (quantitative reverse-transcription PCR)

Total RNA was obtained from cumulus cells and oocytes using RNAqueous Microkit (Ambion) and was treated for genomic DNA contamination using DNase I (Ambion). Reverse transcription was performed using the RETROscript kit (Ambion) in two steps: first, template RNA and oligo(dT) primers were incubated at 85 °C for 3 min to eliminate any secondary structures, and then the buffer and enzyme were added and the reaction was carried out at 42 °C for 1 h. qRT-PCRs were carried out on an iCycler (Bio-Rad Laboratories). cDNA was prepared as described above, and assayed in triplicate. Each experiment was repeated three times using five animals from each genotype. Each 25 μl

reaction contained 12.5 μl of 2× SYBR Green supermix (Bio-Rad Laboratories), 0.4 μM of each primer and 1 μl of template. Expression of the target gene was normalized to β-actin levels. The primers used for real-time PCR reactions are given in Supplementary Table S1. A standard curve for each set of primers was first used to determine the linear dynamic range of each reaction and the PCR efficiency. A melting curve analysis was used to exclude non-specific amplifications. The $2^{-\Delta\Delta C_t}$ (cycle threshold) method was used to calculate relative expression levels. Results were reported as a fold change in gene expression between different genotypes.

Evaluation of cumulus expansion and oocyte retention

Female mice were treated with an intraperitoneal injection of 5 IU of PMSG (Sigma–Aldrich), followed by an injection of 5 IU of hCG (Sigma–Aldrich) given 48 h later. To assess cumulus expansion or oocyte retention, ovaries were isolated 9 or 16 h after hCG stimulation respectively. Ovaries were then fixed in Bouin's solution overnight, dehydrated in ethanol and embedded in paraffin. Serial sections (5 μm thick) were obtained and stained with haematoxylin and periodic acid–Schiff using a standard protocol [26]; every fifth section was evaluated.

Cumulus expansion was assessed using a previously described scoring system [31] (n = 4 mice for each genotype). Every pre-ovulatory (late antral) follicle with a visible nucleus was evaluated for cumulus expansion. Unexpanded complexes received a score of 0 to + 1. Complexes in which the outer layers of cumulus cells had begun to expand received a score of + 2. A score of + 3 was indicative of complexes in which all layers except the corona radiata had expanded, whereas maximally expanded complexes were scored + 4. Evidence of meiotic resumption in oocytes that were in late antral follicle stage was also assessed.

Oocyte retention was assessed as described previously [32] by determining the number of luteinized follicles with or without a retained oocyte (n = 5 mice for each genotype).

Statistical analysis

Statistical analysis was performed using ANOVA for comparisons of multiple groups. For comparison between two groups, Student's t test was used. Statistical significance was defined as $P < 0.05$.

RESULTS

Characterization of *Epab*$^{-/-}$ mice

We generated *Epab*-deficient mice by targeted deletion of the *Epab* gene. Exon 2 of the *Epab* gene, encoding a portion of the first RRM1 domain of full-length EPAB, was replaced by the neomycin resistance gene (*Neo*). The absence of exon 2 from the *Epab* mRNA results in a frameshift and generates a stop codon three amino acids downstream in exon 3 (Figure 1A). The truncated protein contains only part of the first RRM (RRM1) and lacks the remaining three RRMs and the PABC domain of full-length EPAB [17]. The *Epab*-targeting vector was electroporated into ESCs and recombinant ESC colonies were identified by Southern blot analysis for the presence of the 3′-targeting region (Figure 1B), whereas the 5′-targeting region was assessed by genomic PCR (Figure 1C). Targeted ESC clones with homologous recombination were injected into C57BL/6 blastocysts to generate chimaeric mice. Mating chimaeric male mice with C57BL/6 females produced heterozygous offspring. The *Neo* gene was removed by crossing heterozygous mice with the CMV-*Cre* transgenic mice. *Epab*$^{+/-}$ mice were crossed to generate *Epab*$^{-/-}$ mice as confirmed by Southern blot analysis (Supplementary Figure S1A at http://www.BiochemJ.org/bj/446/bj4460047add.htm) and genomic PCR (Supplementary Figure S1B). Production of only

targeted transcripts in *Epab*$^{-/-}$ ovaries was demonstrated using RT–PCR (Figure 1D). These findings confirmed that our targeting strategy successfully disrupted both copies of the *Epab* gene.

Epab-deficient mice are infertile, despite normal oestrous cycle and sexual behaviour

Male and female *Epab*$^{+/-}$ mice appeared phenotypically normal, and inter-crossing of the heterozygous mice produced homozygous *Epab*-deficient mice with a normal Mendelian distribution (77$^{+/+}$:127$^{+/-}$:64$^{-/-}$) and male-to-female ratio (143:125). This indicated that the targeted disruption of *Epab* gene did not cause a significant selective disadvantage with regard to genotype or sex. *Epab*-deficient female mice were viable and exhibited no obvious growth or developmental deficiency (Supplementary Figure S2 at http://www.BiochemJ.org/bj/446/bj4460047add.htm).

To evaluate the reproductive performance of *Epab*$^{+/-}$ and *Epab*$^{-/-}$ female mice, we conducted a continuous mating study using sexually mature female mice (n = 9 for each genotype) and WT male mice of proven fertility. After 20 weeks of mating, there were no pregnancies or deliveries observed in *Epab*$^{-/-}$ female mice, which exhibited normal sexual behaviour (assessed by the presence of a vaginal plug). WT and *Epab*$^{+/-}$ females exhibited normal fertility (Table 1). Male *Epab*$^{+/-}$ and *Epab*$^{-/-}$ mice were similarly assessed by mating to WT females and exhibited normal fertility.

To gain an insight into the aetiology of infertility in females, we evaluated the length of the oestrous cycle of WT and *Epab*$^{-/-}$ mice (n = 5) by vaginal smears collected for 25 consecutive days. *Epab*$^{-/-}$ female mice were similar to WT females and exhibited oestrous cycles of normal length that lasted 4–5 days (Supplementary Table S2 at http://www.BiochemJ.org/bj/446/bj4460047add.htm).

Folliculogenesis in *Epab*$^{-/-}$ mice

We assessed follicle development in the ovaries of unstimulated mature (10–12 weeks old) WT and *Epab*$^{-/-}$ mice (n = 6 for each genotype) by histochemistry. Follicles at all developmental stages were present in the ovaries of mature *Epab*$^{-/-}$ mice (Figure 2B). The number of primordial, primary, early antral and antral follicles did not differ between *Epab*$^{-/-}$ and WT ovaries, whereas *Epab*$^{-/-}$ ovaries had a 3-fold higher number of secondary follicles (Figures 2A and 2C). *Epab*$^{-/-}$ ovaries also contained follicles that housed two oocytes (Supplementary Figures S3A and S3B at http://www.BiochemJ.org/bj/446/bj4460047add.htm), and follicles with only two or three layers of granulosa cells that show the beginnings of premature antrum formation (Supplementary Figures S3C and S3D).

Epab$^{-/-}$ female mice do not generate embryos or mature oocytes

Next, we conducted experiments to determine whether *Epab*$^{-/-}$ females have a defect in oocyte maturation, fertilization, or early pre-implantation embryo development. Specifically, we asked whether generation of immature (GV stage) oocytes, mature (MII) oocytes, or two-cell embryos is altered in *Epab*$^{-/-}$ or *Epab*$^{+/-}$ female mice compared with WT (Figures 3A–3E).

To obtain GV-stage oocytes, mice were stimulated with PMSG, and ovaries were removed 44 h later to collect oocytes by follicular puncture. There was no difference between WT, *Epab*$^{+/-}$ and *Epab*$^{-/-}$ female mice in the number of GV-stage oocytes obtained (n = 6 for each genotype) (Figure 3A).

To obtain MII oocytes, adult WT, *Epab*$^{+/-}$ and *Epab*$^{-/-}$ female mice were superovulated with PMSG followed by hCG 48 h later. MII oocytes were collected from the oviducts 14 h

after the hCG injection (n = 15 for each genotype). In *Epab*$^{-/-}$ mice, we could not detect any mature MII oocytes (Figure 3B). Instead, there were 0–2 oocytes per mice without GVs, but with some fragmentation, that we categorized as MI. In addition, the total number of oocytes collected from *Epab*$^{-/-}$ mice was significantly lower compared with WT and *Epab*$^{+/-}$, suggesting that the ovulation process was also affected. Importantly, oocytes obtained from *Epab*$^{-/-}$ mice displayed morphologic abnormalities, including elongated shapes, pronounced cytoplasmic granularity and abnormal polar-body-like structure (Supplementary Figure S4 at http://www.BiochemJ.org/bj/446/bj4460047add.htm). *Epab*$^{+/-}$ mice did not differ from WT for any of the parameters studied.

To determine whether EPAB is required for fertilization and early embryo development, female mice were placed individually with 12-week old WT males immediately after the hCG injection (n = 10 for each genotype) and two-cell embryos were collected 42 h later. We found that *Epab*$^{-/-}$ female mice did not generate any two-cell embryos, whereas there was no difference between *Epab*$^{+/-}$ and WT (Figure 3C).

Spindle formation and chromosome alignment at the metaphase plate are abnormal in *Epab*$^{-/-}$ oocytes

To further characterize the defect in the maturation of *Epab*$^{-/-}$ oocytes, we performed *in vitro* maturation and assessed chromatin and spindle morphology by immunofluorescence. GV-stage oocytes were collected from WT and *Epab*$^{-/-}$ mice as described above. Upon *in vitro* maturation, we observed that more than 50 % of WT oocytes underwent GVBD within 2 h of isolation, whereas none of the *Epab*$^{-/-}$ oocytes displayed GVBD (Figure 3D). After 18 h, only 16.6 % of the *Epab*$^{-/-}$ oocytes underwent GVBD, compared with approximately 80 % of WT oocytes (Figure 3D). Similarly, although 41.9 %of WT oocytes reached the MII stage after 18 h *in vitro*, none of the *Epab*$^{-/-}$ oocytes completed maturation (Figure 3E).

Chromatin and spindle morphology were assessed by immunostaining with DAPI and an anti-α-tubulin antibody, respectively. Oocytes were assessed at 0, 9 and 18 h of *in vitro* maturation, corresponding to GV, MI and MII stages in WT oocytes respectively. Oocytes from both WT and *Epab*$^{-/-}$ mice had a GV at 0 h (Figure 4A). At 9 h, WT oocytes had their chromosomes aligned on a well-formed spindle (Figure 4B), and at 18 h, two spindles were observed for each WT oocyte: one inside the MII oocyte and the other inside the polar body (Figure 4C). At both 9 h and 18 h, the majority of *Epab*$^{-/-}$ oocytes remained at GV stage (79.1 %) (Figure 4). In the few *Epab*$^{-/-}$ oocytes that underwent GVBD (20.9 %), spindle structure was absent, and the chromosomes were not aligned properly at the metaphase plate at 9 or 18 h (Figure 4). Several abnormal configurations of chromosome and tubulin distribution were observed in the knockout oocytes (Figure 4). These findings indicate that, similar to observations *in vivo*, *Epab*$^{-/-}$ oocytes fail to undergo maturation *in vitro*, and spindle formation and chromosome alignment during meiotic divisions are impaired in *Epab*-deficient mice.

Polyadenylation of maternal genes is suppressed in *Epab*$^{-/-}$ oocytes

Cytoplasmic polyadenylation is a key mechanism by which gene expression is regulated during oocyte maturation. Evidence from the *Xenopus* model suggests that EPAB is required for cytoplasmic polyadenylation and oocyte maturation [20,21]. We therefore hypothesized that the inhibition of oocyte maturation in *Epab*$^{-/-}$ oocytes could be associated with a failure in cytoplasmic polyadenylation of maternally stored mRNAs. We used a ligation-dependent PCR-based poly(A) tail assay [29] to analyse the lengths of the endogenous poly(A) tails of maternally stored mRNAs encoding *Ccnb1*, *c-Mos* and *Dazl*, which are subject to polyadenylation during oocyte maturation [33–35]. *Actb* mRNA was tested as a control as described previously [36].

GV-stage oocytes were obtained from WT and *Epab*$^{-/-}$ ovaries, and poly(A) tail lengths of *Ccnb1*, *c-Mos*, *Dazl* and *Actb* mRNAs were assessed at baseline and following 18 h of *in vitro* maturation. In *Epab*$^{-/-}$ oocytes, no elongation of poly(A) tails on *Ccnb1*, *c-Mos* or *Dazl* mRNAs was observed compared with the normal polyadenylation pattern in WT oocytes (Figure 5A). Poly(A) tail length of a control mRNA, *Actb*, did not change after 18 h of *in vitro* maturation of WT or *Epab*$^{-/-}$ oocytes. Western blot analysis revealed that CCNB1 or DAZL (normalized to actin) did not increase in *Epab*$^{-/-}$ oocytes following 18 h of *in vitro* maturation, unlike the WT, where CCNB1 and DAZL accumulated as described previously [37,38] (Figures 5B and 5C).

We also tested whether the amount of *Ccnb1*, *c-Mos* or *Dazl* mRNA is altered in *Epab*$^{-/-}$ oocytes. *Ccnb1*, *c-Mos* and *Dazl* mRNA expression in *Epab*$^{-/-}$ oocytes determined by qRT-PCR was similar to WT at 0 h (Supplementary Figure S5A at http://www.BiochemJ.org/bj/446/bj4460047add.htm), whereas these transcripts were significantly increased in *Epab*$^{-/-}$ oocytes after 18 h of *in vitro* maturation (Supplementary Figure S5B). Our findings suggest that EPAB is required for polyadenylation and translational activation of maternally derived mRNAs upon oocyte maturation.

In addition, we also observed that the decrease in CPEB1 protein that occurs upon WT oocyte maturation [15] did not occur in *Epab*$^{-/-}$ oocytes (Supplementary Figure S5C).

Microinjection of *Epab* mRNA into *Epab*$^{-/-}$ oocytes does not restore maturation

We then asked whether EPAB is required during the stages of oogenesis prior to the stimulation of oocyte maturation. We therefore tested whether oocyte maturation can be restored by microinjection of *Epab* mRNA into Epab-deficient mouse oocytes at the GV stage. *In vitro* transcribed HA-tagged polyadenylated *Epab* mRNA was microinjected into WT and *Epab*$^{-/-}$ GV-stage oocytes. GVBD and polar body extrusion were recorded at 4 and 18 h after *in vitro* maturation respectively. We observed that none of the injected *Epab*$^{-/-}$ oocytes underwent GVDB, compared with 72.5 and 74.3 % of injected and uninjected WT oocytes respectively (Figure 6A). At 18 h, 40.6 %of injected and 44.3 % uninjected WT oocytes reached the MII stage, whereas none of the *Epab*$^{-/-}$ oocytes (injected or uninjected) completed maturation (Figure 6B). The translation of the microinjected transcript was confirmed by Western blot analysis using an anti-HA antibody (Figure 6C).

Expression of *Pabpc1* mRNA is unchanged in *Epab*$^{-/-}$ oocytes

We also tested whether the expression of the somatic cytoplasmic PABP is altered in *Epab*$^{-/-}$ oocytes compared with WT. Using qRT-PCR, we did not detect a significant difference in *Pabpc1* expression between WT and *Epab*$^{-/-}$ oocytes (Supplementary Figure S6 at http://www.BiochemJ.org/bj/446/bj4460047add.htm).

Ovulation is impaired in *Epab*$^{-/-}$ female mice

Epab$^{-/-}$ mice were not different from WT mice in the number of early antral or antral follicles (Figure 2). However, in *Epab*$^{-/-}$ mice, the total number of oocytes released into the oviduct following hyperstimulation with PMSG and hCG was significantly lower compared with WT and *Epab*$^{+/-}$ mice (Figure 3B), suggesting that, in addition to a defect in oocyte maturation, *Epab*-deficient mice may have impaired ovulation.

We therefore tested whether ovulation was affected in *Epab*$^{-/-}$ mice by determining the rate of oocyte retention and comparing it with WT. Ovaries of hyperstimulated mice were collected 16 h after the hCG injection and serial sections were analysed to determine the total number of corpora lutea in each ovary and to assess each corpus luteum for oocyte retention (Supplementary Figure S7A at http://www.BiochemJ.org/bj/446/

bj4460047add.htm). The total number (Supplementary Figure S7B) and the mean diameter (results not shown) of luteinizing follicles were similar between the two groups. However, more than 50 % of corpora lutea in *Epab*$^{-/-}$ mice retained an oocyte, whereas this ratio was only 10 % in WT ($P < 0.01$, Supplementary Figure S7C).

Cumulus expansion is impaired in *Epab*$^{-/-}$ cumulus oocyte complexes

To gain further insight into the aetiology of defective ovulation in *Epab*$^{-/-}$ mice, we assessed cumulus expansion in WT and *Epab*$^{-/-}$ mice. Ovaries of superovulated mice were collected 9 h after the hCG injection, and COCs were analysed in serial sections stained with Periodic acid–Schiff and haematoxylin. As previously stated (Figure 2), we found no difference in the number of antral follicles between mature WT and *Epab*$^{-/-}$ mice. However, although the majority of COCs in WT ovaries appeared well expanded (Figures 7A and 7B), the degree of COC expansion in *Epab*$^{-/-}$ ovaries was significantly reduced (Figures 7A and 7B), and the cumulus cells surrounding *Epab*$^{-/-}$ oocytes consistently showed an atypical tight structure (Figure 7A). When oocytes in COCs were assessed for meiotic resumption, we found that only a minority of oocytes (32.9 %) in COCs of *Epab*$^{-/-}$ ovaries had undergone GVBD (Supplementary Figure S8 at http://www.BiochemJ.org/bj/446/bj4460047add.htm). Conversely, GVBD had occurred in 99.25 % of oocytes in WT COCs. In addition, the metaphase spindle was also visible in most oocytes in COCs of WT ovaries (Figure 7A). We also measured the diameter of the antral follicles and of the oocytes contained within antral follicles, and found both diameters to be significantly smaller in *Epab*$^{-/-}$ ovaries compared with WT (Figures 7C and 7D).

We then tested whether the expression of genes known to regulate cumulus expansion is altered in *Epab*$^{-/-}$ mice. Ovaries of superovulated mice were collected 4 h after the hCG injection, COCs were obtained by ovarian puncture and cumulus cells were isolated by hyaluronidase treatment. Levels of mRNAs corresponding to *Areg* (amphiregulin), *Ereg* (epiregulin), *Btc* (betacellulin), *Ptgs2* (prostaglandin synthase 2), *Has2* (hyaluronan synthase 2) and *Tnfaip6* (tumour necrosis factor α-induced protein 6) were assessed using qRT-PCR and normalized to β-actin and two additional housekeeping genes, *Tbp* (TATA-binding protein) and *Gapdh* (glyceraldehyde-3-phosphate dehydrogenase), which were found to be unchanged between WT and *Epab*$^{-/-}$ (Supplementary Figure S9 at http://www.BiochemJ.org/bj/446/bj4460047add.htm). We found that the expression of *Areg*, *Ereg*, *Btc*, *Ptgs2*, *Has2* and *Tnfaip6* was significantly reduced in *Epab*$^{-/-}$ mice (Figure 8). Our findings suggest that, in the absence of EPAB, LH-mediated reprogramming of the somatic cells of the pre-ovulatory follicle fails to occur, resulting in impaired cumulus expansion and ovulation.

The effect of the *Epab*-null phenotype on cumulus cells is likely to be indirect

We had previously performed RNA *in situ* hybridization in mouse ovarian sections and shown that the *Epab* transcript is expressed in the oocytes but not in the surrounding cumulus cells [17]. In the present study, we performed qRT-PCR for *Epab* in WT mouse oocytes and cumulus cells and confirmed that the *Epab* transcript is largely absent from cumulus cells (Supplementary Figure S10 at http://www.BiochemJ.org/bj/446/bj4460047add.htm)

DISCUSSION

Analysis of the phenotypic characteristics of mice with targeted disruption of the *Epab* gene indicates that EPAB plays a unique role in oocyte and follicle development. *Epab*-deficient females are infertile, and display impaired oocyte maturation as well as ovulation. Molecular characterization of reproductive defects in knockout mice reveals that *Epab*-deficient

oocytes fail to achieve translational activation of mRNAs upon stimulation of oocyte maturation. The defect in ovulation is associated with impaired cumulus expansion and a significant down-regulation of mRNAs encoding the EGF (epidermal growth factor)-like growth factors, *Areg*, *Ereg* and *Btc*, and their downstream regulators, *Ptgs2*, *Has2* and *Tnfaip6*. The absence of *Epab* also affects earlier stages of oogenesis and folliculogenesis, as the microinjection of *Epab* into GV-stage *Epab*$^{-/-}$ oocytes does not restore maturation and ovaries of *Epab*$^{-/-}$ mice have a significantly higher number of secondary follicles.

Resumption of meiosis in oocytes arrested at the diplotene stage of the first meiotic division requires activation of MPF (maturation-promotion factor) [39], a heterodimer composed of CDK1 (cyclin-dependent kinase 1, also known as CDC2) [40] and cyclin B1 [41]. During this first meiotic (G2) arrest, phosphorylation of CDC2 at Thr^{14} and Thr^{15} (by Wee1B and Myt1) results in inactivation of the CDC2–cyclin B1 complex (MPF) in mouse [42–45]. Activation of CDC2 (and therefore meiotic resumption) is controlled at several steps, including dephosphorylation of CDC2 at Thr^{14} and Thr^{15} by CDC25B and phosphorylation at Thr^{161} by the CAK (CDK-activating kinase) complex [46,47]. In addition, upon stimulation of oocyte maturation, *Ccnb1* mRNA undergoes translational activation by cytoplasmic polyadenylation [34] and cyclin B1 protein concentration increases in the oocyte [37,38]. In mouse oocytes, cyclin B1 controls the formation of the first meiotic spindle and progression of meiotic maturation [34,48]. Our findings demonstrate that EPAB is required for cytoplasmic polyadenylation and translational activation of mRNAs upon stimulation of oocyte maturation, including *Ccnb1* mRNA (Figure 5).

Once transcriptional activity is suppressed in the oocyte, distinct pathways are activated in a transcript-specific and temporal manner to meet the changing needs of the oocyte and the early embryo [13]. To date, two such pathways have been identified in the *Xenopus* model: CPEB1/SYMPK/CPSF [20] and Pumilio/Dazl [14]. Both are regulated by oocyte-specific protein complexes that bind conserved sequences on the 3′-UTR (3′-untranslated region) of mRNAs [14,49,50]. The roles of CPEB and DAZL, key regulators of these pathways, have been characterized in the mouse using genetic approaches. Both *Cpeb*-null and *Dazl*-null female mice are infertile with vestigial ovaries that are devoid of oocytes, owing to loss of oocytes during embryonic development [51–53], suggesting a role for both factors during the early stages of oogenesis. To study the role of CPEB in later stages of oocyte development, Racki and Richter [54] generated a transgenic mouse expressing siRNA (small interfering RNA) targeting CPEB under the control of the zona pellucida 3 (Zp3) promoter. In these mice, *Mos* mRNA polyadenylation was suppressed, and oocytes underwent maturation and displayed parthenogenesis [54], similar to *Mos*-null mice [55,56]. Similarly, the role of DAZL in later stages of oocyte development was studied by microinjecting GV-stage mouse oocytes with morpholino oligonucletides against *Dazl*. Although a polar body was extruded in 35 %of injected oocytes, spindle formation, chromosome condensation and congression were impaired and fertilization did not occur [15].

Our findings demonstrate that the absence of EPAB results in complete maturation arrest in mouse oocytes (Figures 3 and 4). This is not surprising for multiple reasons. First, EPAB has been identified within both known complexes of translational activation in *Xenopus* oocytes [14,20]. Secondly, we have recently reported that phosphorylation at a four residue cluster of *Xenopus* EPAB is required for cytoplasmic polyadenylation and oocyte maturation [21]. Finally, in mouse, the *Epab*-null phenotype is associated with deregulation of both DAZL (Figure 5) and CPEB (Supplementary Figure S5C) protein expression. Importantly, we found that the maturation defect in *Epab*$^{-/-}$ oocytes is not rescued by the expression of EPAB in GV-stage oocytes. Therefore, EPAB seems to be required for stages of oocyte development prior to the stimulation of oocyte maturation, a finding consistent with prior

studies demonstrating that blocking translation does not inhibit GVBD in mouse oocytes [57].

In mammals, the LH surge results in a cascade of events in ovarian pre-ovulatory follicles that is necessary for the ovulation of a fertilizable oocyte. AREG, EREG and BTC (encoded by *Areg*, *Ereg* and *Btc* respectively) are members of the EGF-like family that are up-regulated by LH in granulosa [58–60] and cumulus cells [61] and mediate paracrine actions of LH within the follicle. *In vitro*, AREG, EREG and BTC each induce the expression of *Ptgs2* [prostaglandin synthase-2 or COX2 (cyclooxygenase-2)], *Tnfaip6* (TNFAIP6) and *Has2* (HAS2) [58], genes that are necessary for synthesis and stabilization of the extracellular matrix by cumulus cells and required for cumulus expansion [62–65]. Although, in mouse ovaries, *Epab* mRNA is exclusively expressed in oocytes [17] (Supplementary Figure S10), we found that EPAB is necessary for the up-regulation of the mRNAs encoding *Areg*, *Ereg* and *Btc*, and their downstream mediators *Ptgs2*, *Tnfaip6* and *Has2* (Figure 8), as well as cumulus expansion (Figure 7) and ovulation (Supplementary Figure S7), an effect that has not been reported for *Cpeb*- or *Dazl*-null phenotypes [15,54]. It is also noteworthy that the targeted deletion of *Pde3A*, which is also exclusively expressed in oocytes, results only in maturation arrest, without affecting cumulus expansion or ovulation [66].

Overall, our findings establish EPAB as a key factor required for mouse oocyte and follicle development. Similar to that observed in *Xenopus* [21], EPAB mediates translational activation of gene expression by cytoplasmic polyadenylation and maturation in mouse oocytes. In addition, in the mouse model, EPAB is required for pre-ovulatory changes in the follicle and for ovulation. The role of EPAB in earlier stages of oocyte and follicle development remains to be characterized further. In addition, gene groups regulated by EPAB at different stages of oogenesis and folliculogenesis, and proteins that form complexes with EPAB in the mammalian oocyte, remain to be identified.

Supplementary Material

Refer to Web version on PubMed Central for supplementary material.

Acknowledgments

We thank Joan A. Steitz for critically reading the paper prior to submission.

FUNDING

This project was supported by the National Institutes of Health (NIH) [grant numbers K08 HD046581-01 and R01HD059909 (to E.S.)]. M.D.L. was supported by the National Center for Advancing Translational Sciences (NCATS) [CTSA grant number UL1 RR024139], a component of the NIH, and NIH Roadmap for Medical Research.

Abbreviations used

AREG	amphiregulin
BTC	betacellulin
CDK	cyclin-dependent kinase
COC	cumulus–oocyte complex
CPE	cytoplasmic polyadenylation element
CPEB1	CPE-binding protein 1

CPSF	cytoplasmic polyadenylation specificity factor
DAPI	4′,6-diamidino-2-phenylindole
DAZL	deleted in azoospermia-like
EGF	epidermal growth factor
EPAB	embryonic poly(A)-binding protein
EREG	epiregulin
ESC	embryonic stem cell
FBS	fetal bovine serum
FSH	follicle-stimulating hormone
GV	germinal vesicle
GVBD	GV breakdown
HA	haemagglutinin
HAS2	hyaluronan synthase 2
hCG	human chorionic gonadotropin
IBMX	isobutylmethylxanthine
LH	luteinizing hormone
MPF	maturation-promotion factor
PABP	poly(A)-binding protein
PABPC1	PABP cytoplasmic 1
PMSG	pregnant mare serum gonadotropin
PTGS2	prostaglandin synthase 2
qRT-PCR	quantitative reverse-transcription PCR
RRM	RNA-recognition motif
RT	reverse transcription
SYMPK	symplekin
TNFAIP6	tumour necrosis factor α-induced protein 6
WT	wild-type
ZGA	zygotic gene activation

References

1. Eppig JJ. Oocyte-somatic cell communication in the ovarian follicles of mammals. Semin Dev Biol. 1994; 5:51–59.
2. Adashi EY. Endocrinology of the ovary. Hum Reprod. 1994; 9:815–827. [PubMed: 7929728]
3. Hsieh M, Zamah AM, Conti M. Epidermal growth factor-like growth factors in the follicular fluid: role in oocyte development and maturation. Semin Reprod Med. 2009; 27:52–61. [PubMed: 19197805]
4. Diaz FJ, Wigglesworth K, Eppig JJ. Oocytes determine cumulus cell lineage in mouse ovarian follicles. J Cell Sci. 2007; 120:1330–1340. [PubMed: 17389684]

5. Matova N, Cooley L. Comparative aspects of animal oogenesis. Dev Biol. 2001; 231:291–320. [PubMed: 11237461]
6. Eppig JJ. Intercommunication between mammalian oocytes and companion somatic cells. BioEssays. 1991; 13:569–574. [PubMed: 1772412]
7. Richards JS, Russell DL, Ochsner S, Espey LL. Ovulation: new dimensions and new regulators of the inflammatory-like response. Annu Rev Physiol. 2002; 64 :69–92. [PubMed: 11826264]
8. Radford HE, Meijer HA, de Moor CH. Translational control by cytoplasmic polyadenylation in *Xenopus* oocytes. Biochim Biophys Acta. 2008; 1779:217–229. [PubMed: 18316045]
9. Hake LE, Richter JD. CPEB is a specificity factor that mediates cytoplasmic polyadenylation during *Xenopus* oocyte maturation. Cell. 1994; 79:617–627. [PubMed: 7954828]
10. Gebauer F, Richter JD. Mouse cytoplasmic polyadenylylation element binding protein: an evolutionarily conserved protein that interacts with the cytoplasmic polyadenylylation elements of c-mos mRNA. Proc Natl Acad Sci USA. 1996; 93:14602–14607. [PubMed: 8962099]
11. Stebbins-Boaz B, Hake LE, Richter JD. CPEB controls the cytoplasmic polyadenylation of cyclin, Cdk2 and c-mos mRNAs and is necessary for oocyte maturation in *Xenopus*. EMBO J. 1996; 15:2582–2592. [PubMed: 8665866]
12. Barnard DC, Ryan K, Manley JL, Richter JD. Symplekin and xGLD-2 are required for CPEB-mediated cytoplasmic polyadenylation. Cell. 2004; 119:641–651. [PubMed: 15550246]
13. Vasudevan S, Seli E, Steitz JA. Metazoan oocyte and early embryo development program: a progression through translation regulatory cascades. Genes Dev. 2006; 20 :138–146. [PubMed: 16418480]
14. Padmanabhan K, Richter JD. Regulated Pumilio-2 binding controls RINGO/Spy mRNA translation and CPEB activation. Genes Dev. 2006; 20:199–209. [PubMed: 16418484]
15. Chen J, Melton C, Suh N, Oh JS, Horner K, Xie F, Sette C, Blelloch R, Conti M. Genome-wide analysis of translation reveals a critical role for deleted in azoospermia-like (Dazl) at the oocyte-to-zygote transition. Genes Dev. 2011; 25:755–766. [PubMed: 21460039]
16. Voeltz GK, Ongkasuwan J, Standart N, Steitz JA. A novel embryonic poly(A) binding protein, ePAB, regulates mRNA deadenylation in *Xenopus* egg extracts. Genes Dev. 2001; 15:774–788. [PubMed: 11274061]
17. Seli E, Lalioti MD, Flaherty SM, Sakkas D, Terzi N, Steitz JA. An embryonic poly(A)-binding protein (ePAB) is expressed in mouse oocytes and early preimplantation embryos. Proc Natl Acad Sci USA. 2005; 102:367–372. [PubMed: 15630085]
18. Wilkie GS, Gautier P, Lawson D, Gray NK. Embryonic poly(A)-binding protein stimulates translation in germ cells. Mol Cell Biol. 2005; 25:2060–2071. [PubMed: 15713657]
19. Guzeloglu-Kayisli O, Pauli SA, Demir H, Lalioti MD, Sakkas D, Seli E. Identification and characterization of human embryonic poly(A) binding protein (ePAB). Mol Hum Reprod. 2008; 14:581–588. [PubMed: 18716053]
20. Kim JH, Richter JD. RINGO/cdk1 and CPEB mediate poly(A) tail stabilization and translational regulation by ePAB. Genes Dev. 2007; 21:2571–2579. [PubMed: 17938241]
21. Friend JK, Brook ML, Bezirci FB, Sheets MD, Gray NR, Seli E. Embryonic poly(A)-binding protein (ePAB) phosphorylation is required for *Xenopus* oocyte maturation. Biochem J. 2012; 445:93–100. [PubMed: 22497250]
22. Ozturk S, Guzeloglu-Kayisli O, Demir N, Sozen B, Ilbay O, Lalioti MD, Seli E. Epab and Pabpc1 are differentially expressed during male germ cell development. Reprod Sci. 201210.1177/1933719112446086
23. Flach G, Johnson MH, Braude PR, Taylor RA, Bolton VN. The transition from maternal to embryonic control in the 2-cell mouse embryo. EMBO J. 1982; 1:681–686. [PubMed: 7188357]
24. Pasparakis M, Courtois G, Hafner M, Schmidt-Supprian M, Nenci A, Toksoy A, Krampert M, Goebeler M, Gillitzer R, Israel A, et al. TNF-mediated inflammatory skin disease in mice with epidermis-specific deletion of IKK2. Nature. 2002; 417:861–866. [PubMed: 12075355]
25. Sauer B. Inducible gene targeting in mice using the Cre/lox system. Methods. 1998; 14:381–392. [PubMed: 9608509]
26. Sheehan, DC.; Hrapchak, BB. Theory and Practice of Histotechnology. 2. Battelle Memorial Institute; Columbus, OH: 1987.

27. Mehlmann LM, Saeki Y, Tanaka S, Brennan TJ, Evsikov AV, Pendola FL, Knowles BB, Eppig JJ, Jaffe LA. The Gs-linked receptor GPR3 maintains meiotic arrest in mammalian oocytes. Science. 2004; 306:1947–1950. [PubMed: 15591206]
28. Goldman JM, Murr AS, Cooper RL. The rodent estrous cycle: characterization of vaginal cytology and its utility in toxicological studies. Birth Defects Res, Part B. 2007; 80:84–97.
29. Salles FJ, Strickland S. Rapid and sensitive analysis of mRNÁ polyadenylation states by PCR. PCR Methods Appl. 1995; 4:317–321. [PubMed: 7580923]
30. Kline D. Quantitative microinjection of mouse oocytes and eggs. Methods Mol Biol. 2009; 518:135–156. [PubMed: 19085140]
31. Vanderhyden BC, Caron PJ, Buccione R, Eppig JJ. Developmental pattern of the secretion of cumulus expansion-enabling factor by mouse oocytes and the role of oocytes in promoting granulosa cell differentiation. Dev Biol. 1990; 140:307–317. [PubMed: 2115479]
32. White R, Leonardsson G, Rosewell I, Ann Jacobs M, Milligan S, Parker M. The nuclear receptor co-repressor nrip1 (RIP140) is essential for female fertility. Nat Med. 2000; 6:1368–1374. [PubMed: 11100122]
33. Gebauer F, Xu W, Cooper GM, Richter JD. Translational control by cytoplasmic polyadenylation of c-mos mRNA is necessary for oocyte maturation in the mouse. EMBO J. 1994; 13:5712–5720. [PubMed: 7988567]
34. Tay J, Hodgman R, Richter JD. The control of cyclin B1 mRNA translation during mouse oocyte maturation. Dev Biol. 2000; 221:1–9. [PubMed: 10772787]
35. Huarte J, Stutz A, O'Connell ML, Gubler P, Belin D, Darrow AL, Strickland S, Vassalli JD. Transient translational silencing by reversible mRNA deadenylation. Cell. 1992; 69:1021–30. [PubMed: 1606611]
36. Nakanishi T, Kubota H, Ishibashi N, Kumagai S, Watanabe H, Yamashita M, Kashiwabara SI, Miyado K, Baba T. Possible role of mouse poly(A) polymerase mGLD-2 during oocyte maturation. Dev Biol. 2006; 289:115–126. [PubMed: 16325797]
37. Hampl A, Eppig JJ. Translational regulation of the gradual increase in histone H1 kinase activity in maturing mouse oocytes. Mol Reprod Dev. 1995; 40:9–15. [PubMed: 7702874]
38. Winston NJ. Stability of cyclin B protein during meiotic maturation and the first mitotic cell division in mouse oocytes. Biol Cell. 1997; 89:211–219. [PubMed: 9429304]
39. Masui Y, Markert CL. Cytoplasmic control of nuclear behavior during meiotic maturation of frog oocytes. J Exp Zool. 1971; 177:129–145. [PubMed: 5106340]
40. Gautier J, Norbury C, Lohka M, Nurse P, Maller J. Purified maturation promoting factor contains the product of a *Xenopus* homolog of the fission yeast cell cycle control gene cdc2 + Cell. 1988; 54:433–439. [PubMed: 3293803]
41. Gautier J, Minshull J, Lohka M, Glotzer M, Hunt T, Maller JL. Cyclin is a component of maturation-promoting factor from *Xenopus*. Cell. 1990; 60:487–494. [PubMed: 1967981]
42. Lundgren K, Walworth N, Dembski M, Kirschner M, Beach D. mik1 and wee1 cooperate in the inhibitory tyrosine phosphorylation of cdc2. Cell. 1991; 64:1111–1122. [PubMed: 1706223]
43. Parker LL, Piwnica-Worms H. Inactivation of the p34cdc2-Cyclin B complex by the human WEE 1 tyrosine kinase. Science. 1992; 257:1955–1957. [PubMed: 1384126]
44. Mueller PR, Coleman TR, Kumagai A, Dunphy WG. Myt1: a membrane-associated inhibitory kinase that phosphorylates Cdc2 on both threonine-14 and tyrosine-15. Science. 1995; 270:86–90. [PubMed: 7569953]
45. Wells NJ, Watanabe N, Tokusumi T, Jiang W, Verdecia MA, Hunter T. The C-terminal domain of the Cdc2 inhibitory kinase Myt1 interacts with Cdc2 complexes and is required for inhibition of G_2/M progression. J Cell Sci. 1999; 112:3361–3371. [PubMed: 10504341]
46. Fesquet D, Labbé JC, Derancourt J, Capony JP, Galas S, Girard F, Lorca T, Shuttleworth J, Doree M, Cavadore JC. The MO15 gene encodes thé catalytic subunit of a protein kinase that activates cdc2 and other cyclin-dependent kinases (CDKs) through phosphorylation of Thr161 and its homologues. EMBO J. 1993; 12:3111–3121. [PubMed: 8344251]
47. Solomon MJ, Harper JW, Shuttleworth J. CAK, the p34cdc2 activating kinase, contains a protein identical or closely related to p40MO15. EMBO J. 1993; 12:3133–3142. [PubMed: 8344252]

48. Polanski Z, Ledan E, Brunet S, Louvet S, Kubiak JZ, Verlhac MH, Maro B. Cyclin synthesis controls the progression of meiotic maturation in mouse oocytes. Development. 1998; 125:4989–4997. [PubMed: 9811583]
49. de Moor CH, Meijer H, Lissenden S. Mechanisms of translational control by the 3′UTR in development in development and differentiation. Semin Cell Dev Biol. 2005; 16 :49–58. [PubMed: 15659339]
50. Piccioni F, Zappavigna V, Verotti AC. Translational regulation during oogenesis and early development: the cap-poly(A) tail relationship. C R Biol. 2005; 328:863–881. [PubMed: 16286077]
51. Tay J, Richter JD. Germ cell differentiation and synaptonemal complex formation are disrupted in CPEB knockout mice. Dev Cell. 2001; 1:201–213. [PubMed: 11702780]
52. Ruggiu M, Speed R, Taggart M, McKay SJ, Kilanowski F, Saunders P, Dorin J, Cooke HJ. The mouse Dazla gene encodes a cytoplasmic protein essential for gametogenesis. Nature. 1997; 389:73–77. [PubMed: 9288969]
53. Lin Y, Page DC. Dazl deficiency leads to embryonic arrest of germ cell development in XY C57BL/6 mice. Dev Biol. 2005; 288:309–316. [PubMed: 16310179]
54. Racki WJ, Richter JD. CPEB controls oocyte growth and follicle development in the mouse. Development. 2006; 133:4527–4537. [PubMed: 17050619]
55. Colledge WH, Carlton MBL, Udy GB, Evans MJ. Disruption of c-mos causes parthenogenetic development of unfertilized mouse eggs. Nature. 1994; 370:65–67. [PubMed: 8015609]
56. Hashimoto N, Watanabe N, Furuta Y, Tamemoto H, Sagata N, Yokoyama M, Okazaki K, Nagayoshi M, Takeda N, Ikawa Y, Aizawa S. Parthenogenetic activation of oocytes in c-mos-deficient mice. Nature. 1994; 370:68–71. [PubMed: 8015610]
57. Wassarman PM, Josefowicz WJ, Letourneau GE. Meiotic maturation of mouse oocytes *in vitro*: inhibition of maturation at specific stages of nuclear progression. J Cell Sci. 1976; 22:531–545. [PubMed: 190244]
58. Park JY, Su YQ, Ariga M, Law E, Jin SL, Conti M. EGF-like growth factors as mediators of LH action in the ovulatory follicle. Science. 2004; 303:682–684. [PubMed: 14726596]
59. Sekiguchi T, Mizutani T, Yamada K, Kajitani T, Yazawa T, Yoshino M, Miyamoto K. Expression of epiregulin and amphiregulin in the rat ovary. J Mol Endocrinol. 2004; 33:281–291. [PubMed: 15291759]
60. Freimann S, Ben-Ami I, Dantes A, Ron-El R, Amsterdam A. EGF-like factor epiregulin and amphiregulin expression is regulated by gonadotropins/cAMP in human ovarian follicular cells. Biochem Biophys Res Commun. 2004; 324:829–834. [PubMed: 15474502]
61. Shimada M, Hernandez-Gonzalez I, Gonzalez-Robayna I, Richards JS. Paracrine and autocrine regulation of epidermal growth factor-like factors in cumulus oocyte complexes and granulosa cells: key roles for prostaglandin synthase 2 and progesterone receptor. Mol Endocrinol. 2006; 20:1352–1365. [PubMed: 16543407]
62. Dinchuk JE, Car BD, Focht RJ, Johnston JJ, Jaffee BD, Covington MB, Contel NR, Eng VM, Collins RJ, Czerniak PM, et al. Renal abnormalities and an altered inflammatory response in mice lacking cyclooxygenase II. Nature. 1995; 378:406–409. [PubMed: 7477380]
63. Davis BJ, Lennard DE, Lee CA, Tiano HF, Morham SG, Wetsel WC, Langenbach R. Anovulation in cyclooxygenase-2-deficient mice is restored by prostaglandin E2 and interleukin-1β. Endocrinology. 1999; 140:2685–2695. [PubMed: 10342859]
64. Ochsner SA, Day AJ, Rugg MS, Breyer RM, Gomer RH, Richards JS. Disrupted function of tumor necrosis factor-α-stimulated gene 6 blocks cumulus celloocyte complex expansion. Endocrinology. 2003; 144:4376–4384. [PubMed: 12959984]
65. Fülöp C, Szántó S, Mukhopadhyay D, Bárdos T, Kamath RV, Rugg MS, Day AJ, Salustri A, Hascall VC, Glant TT, Mikecz K. Impaired cumulus mucification and female sterility in tumor necrosis factor-induced protein-6 deficient mice. Develoment. 2003; 130:2253–2261.
66. Masciarelli S, Horner K, Liu C, Park SH, Hinckley M, Hockman S, Nedachi T, Jin C, Conti M, Manganiello V. Cyclic nucleotide phosphodiesterase 3A-deficient mice as a model of female infertility. J Clin Invest. 2004; 114:196–205. [PubMed: 15254586]

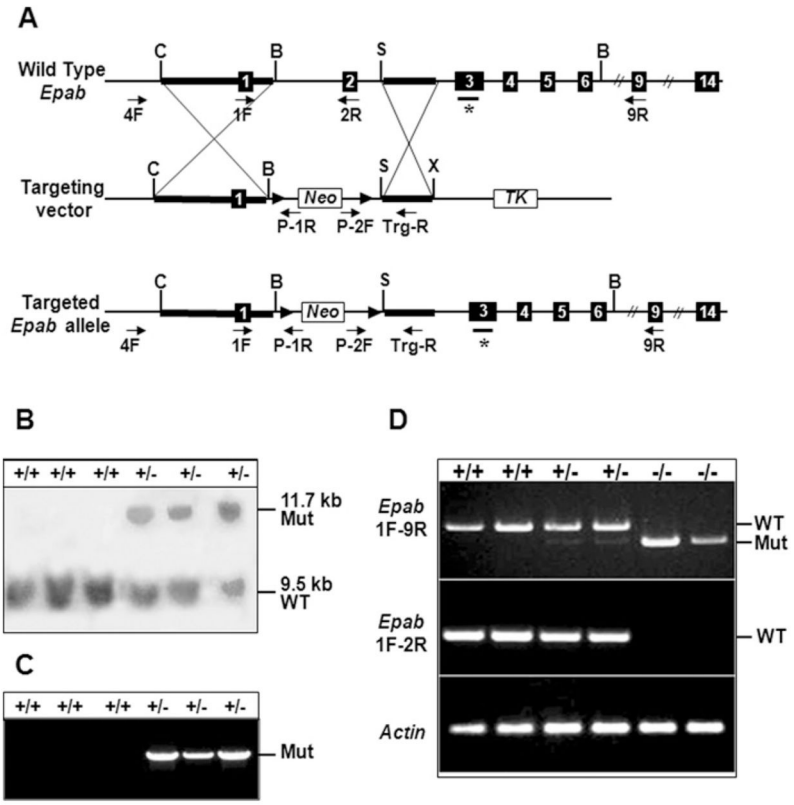

Figure 1. Generation of *Epab*-deficient mice

(**A**) Schematic representation of: the genomic organization of mouse *Epab* (top panel); the targeting construct engineered in pEZ-Flox (middle panel); and the targeted *Epab* allele (bottom panel). Exons are indicated by numbered and filled boxes. Expected sites of homologous recombination are shown with straight lines. * indicates the 3′-probe used for Southern blot analysis. Arrows show the location of PCR primers. Arrowheads depict LoxP sites. Restriction sites are indicated as C for ClaI, B for BamHI, S for SalI and X for XhoI. *Neo*, neomycin gene; *TK* , thymidine kinase gene. (**B**) Southern blot analysis of WT (+/+ , first three lanes) and $Epab^{+/-}$ (+/− , last three lanes) ES cells. BamHI digestion and hybridization with the exon 3 probe detected a 9.5 kb band and an 11.7 kb band for the WT and mutant (Mut) alleles respectively. (**C**) PCR analysis of genomic DNA extracted from ES cells. A 5.6 kb fragment is amplified from the mutant (Mut) allele using the 4F primer located in the *Epab* gene and the P-1R primer located in the targeting vector. (**D**) *Epab* RT–PCR analysis in WT (+/+, $Epab^{+/-}$ (+/−), and $Epab^{-/-}$ (−/−) mouse ovaries. PCR with primers 1F (exon 1) and 9R (exon 9) amplified a 1.2 kb and a 1 kb fragments from the WT and the mutant (Mut) alleles respectively. PCR with primers on exons 1–2 only amplified a fragment from the WT allele. Actin RT–PCR was used as an internal control.

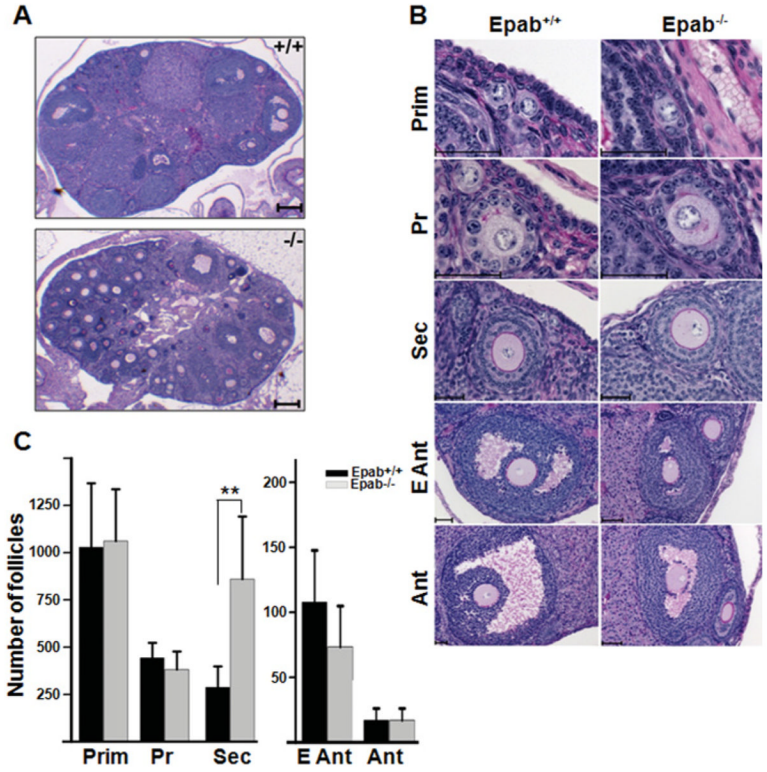

Figure 2. Histomorphometric evaluation of *Epab*$^{-/-}$ ovaries

Follicle development was assessed in ovaries of unstimulated mature (10–12 weeks old) WT and *Epab*$^{-/-}$ mice. (**A**) Representative low-magnification micrographs of ovaries from 12-week-old WT (+/+) and *Epab*$^{-/-}$ (−/−) mice. Scale bars represent 10 μm. (**B**) Representative high-magnification micrographs of follicles from 12-week-old WT (*Epab*$^{+/+}$) and *Epab*$^{-/-}$ mice at different developmental stages. Prim: primordial; Pr: primary; Sec: secondary; E Ant: early antral; Ant: antral follicles. Scale bars represent 10 μm. (**C**) Follicular count of unstimulated ovaries from 10–12-week-old WT (black bars) and *Epab*$^{-/-}$ (grey bars) mice. Follicle counts were conducted using six ovaries of each genotype. Data represent means ± S.E.M. The number of secondary follicles was significantly higher in *Epab*$^{-/-}$ mice; $^{**}P < 0.01$.

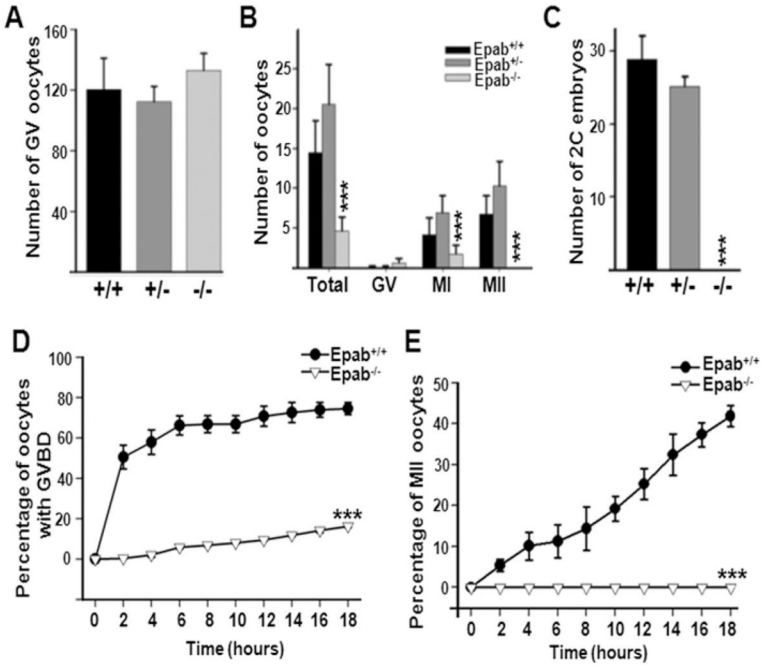

Figure 3. *Epab*-deficient female mice do not generate embryos or mature (MII) oocytes

(**A**) GV-stage oocytes were obtained from the ovaries of 10–12-weeks-old WT ($Epab^{+/+}$), $Epab^{+/-}$ or $Epab^{-/-}$ mice 44 h after stimulation with 5 IU of PMSG ($n = 6$ for each group). There was no difference between $Epab^{+/+}$ (black bar), $Epab^{+/-}$ (dark grey bar) and $Epab^{-/-}$ (light grey bar) mice in the number of GV-stage oocytes obtained. The results represent means ± S.E.M. (**B**) Mature (MII) oocytes were collected from the oviducts of superovulated 10–12-week-old WT ($Epab^{+/+}$), $Epab^{+/-}$ or $Epab^{-/-}$ mice ($n = 15$ for each group). $Epab^{-/-}$ mice (light grey bars) had significantly lower MI and MII oocytes compared with $Epab^{+/+}$ (black bars) or $Epab^{+/-}$ (dark grey bars) mice. In addition, the total number of oocytes found in the oviducts of $Epab^{-/-}$ mice was significantly lower. Results are presented as means ± S.E.M.; ***$P < 0.001$ for $Epab^{-/-}$ compared with $Epab^{+/-}$ or $Epab^{+/+}$ mice. (**C**) Two-cell embryos were collected from the oviducts of superovulated 10–12-week-old WT ($Epab^{+/+}$), $Epab^{+/-}$ or $Epab^{-/-}$ female mice ($n = 10$ for each group) mated with 12-week-old fertile WT males. $Epab^{-/-}$ mice did not produce two-cell embryos, whereas the number of two-cell embryos collected from $Epab^{+/-}$ mice (dark grey bar) was similar to $Epab^{+/+}$ (black bar). Results are presented as means ± S.E.M.; ***$P < 0.001$. (**D**) Assessment of GVBD (consistent with metaphase I stage). GV-stage oocytes were collected from PMSG-primed WT and $Epab^{-/-}$ mice ($n = 4$ mice for each genotype) and cultured under *in vitro* maturation conditions. A total of 135 $Epab^{+/+}$ and 225 $Epab^{-/-}$ oocytes were assessed. The results are presented as means ± S.E.M. At 18 h, only 16.5 % of $Epab^{-/-}$ oocytes completed GVBD compared with 74.5 % of $Epab^{+/+}$; ***$P < 0.001$. (**E**) Assessment of maturation [consistent with metaphase II (MII) stage] described as GVBD and the appearance of a polar body in WT and $Epab^{-/-}$ oocytes cultured under *in vitro* maturation conditions (as described for **D**). At 18 h, 0 % of $Epab^{-/-}$ oocytes had completed maturation compared with 41.9 % of $Epab^{+/+}$; ***$P < 0.001$.

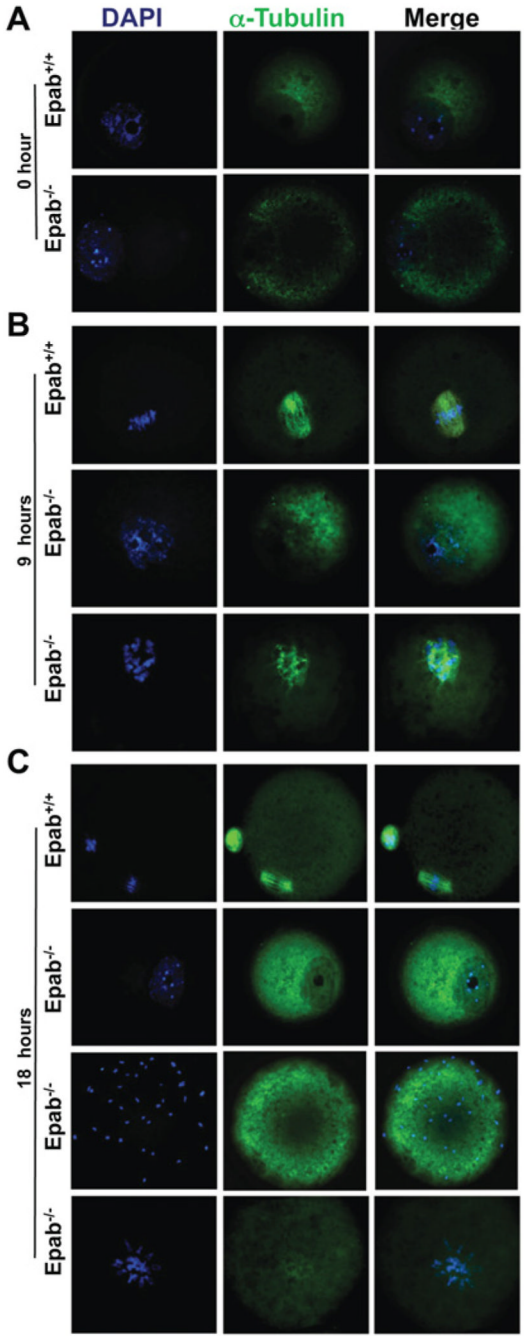

Figure 4. *Epab* is required for meiotic division and chromosome alignment

GV-stage oocytes were collected from PMSG-primed WT and *Epab*$^{-/-}$ mice (n = 4 mice for each genotype). Oocytes were analysed at baseline (0 h) (**A**), or after 9 h (**B**) or 18 h (**C**) of culture under *in vitro* maturation conditions. Column 1, DAPI (blue); Column 2, anti-α-tubulin antibody (green); Column 3, merged images of DAPI and anti-α-tubulin staining. (**A**) At baseline, both WT (*Epab*$^{+/+}$) and *Epab*$^{-/-}$ oocytes have intact nuclear membranes, consistent with GV stage. (**B**) At 9 h, most WT (*Epab*$^{+/+}$) oocytes underwent GVBD, with chromosomes aligned on the spindle, consistent with MI stage, whereas most *Epab*$^{-/-}$ oocytes remained at GV stage. In the small number of *Epab*$^{-/-}$ oocytes with GVBD,

microtubule-like structures (stained with anti-α-tubulin) could be visualized. (**C**) At 18 h, those WT (*Epab*$^{+/+}$) oocytes that reached MII had their chromosomes aligned on the spindle within the oocyte and in the polar body. Most Epab$^{-/-}$ oocytes remained at GV stage, whereas some had disseminated chromosomes, and others showed chromosomes that remained in the centre of the oocytes without microtubule formation.

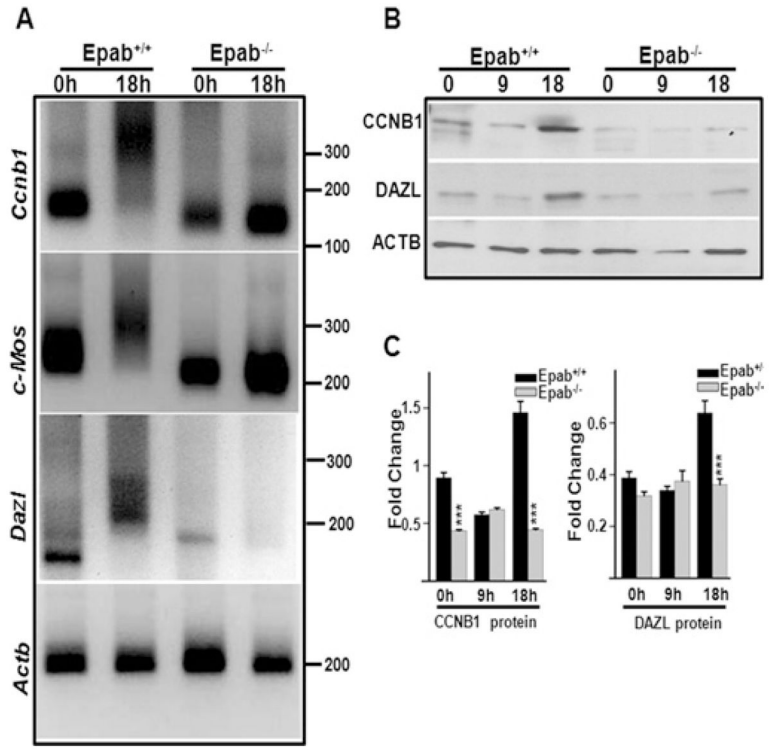

Figure 5. *Epab* is required for cytoplasmic polyadenylation of *Dazl*, *Ccnb1* and *c-Mos* mRNAs

(**A**) GV-stage oocytes were isolated from WT (*Epab*$^{+/+}$) and *Epab*$^{-/-}$ mice and total RNA was isolated from 100 oocytes for each genotype at baseline (0 h) and after 18 h of *in vitro* maturation. Poly(A)-tail lengths were determined using a PCR-based poly(A) tail assay. In *Epab*$^{-/-}$ oocytes, poly(A)-tail lengths of *Ccnb1*, *c-Mos* or *Dazl* mRNAs did not increase upon 18 h of *in vitro* maturation, whereas a >100 bp increase was observed in WT. *ACTB* mRNA was polyadenylated prior to oocyte maturation and maintained poly(A)-tail length in both WT and *Epab*$^{-/-}$ oocytes. (**B** and **C**) GV-stage oocytes were collected from PMSG-primed WT (*Epab*$^{+/+}$) and *Epab*$^{-/-}$ mice and cultured for *in vitro* maturation. Oocytes were collected at baseline (0 h), after 9 h or 18 h of culture under *in vitro* maturation conditions. CCNB1 and DAZL protein expression were determined with Western blotting and normalized to actin. In *Epab*$^{-/-}$ oocytes, CCNB1 and DAZL protein expression did not increase upon 18 h of *in vitro* maturation compared with a significant increase observed in WT. Results are presented as means ± S.E.M.; ***$P < 0.001$ for *Epab*$^{-/-}$ compared with *Epab*$^{+/+}$ mice.

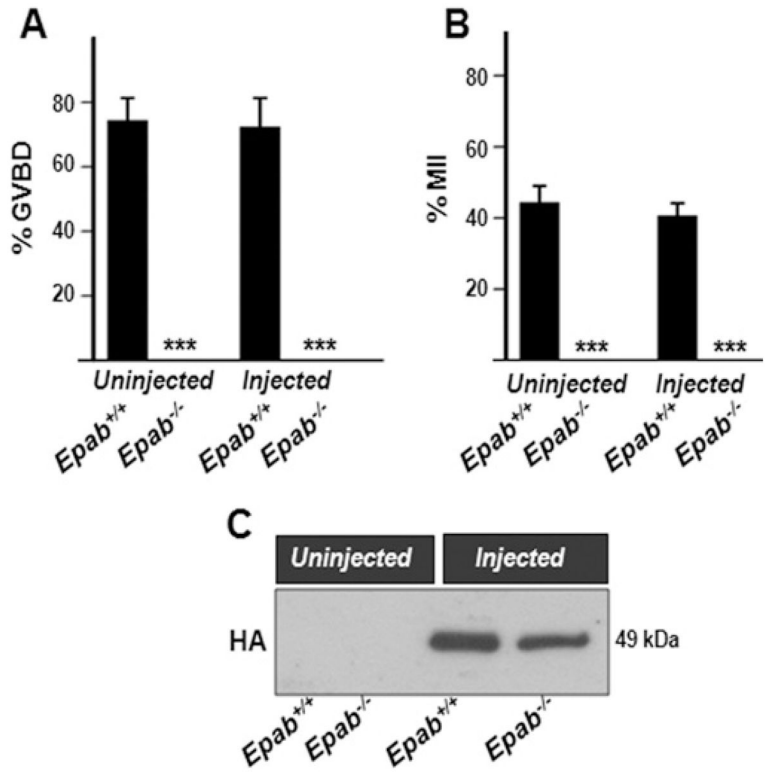

Figure 6. Microinjection of *Epab* mRNA into *Epab*$^{-/-}$ oocytes does not rescue oocyte maturation

(**A**) GV-stage oocytes collected from PMSG-primed WT or Epab$^{-/-}$ mice (n = 4 mice for each genotype) were microinejected with HA-tagged *Epab* mRNA. Uninjected controls were co-cultured for each group. Following overnight culture in milrinone-containing medium, the next day the oocytes were washed and cultured under *in vitro* maturation conditions, and evaluated for GVBD at 4 h. *Epab* mRNA-injected or uninjected *Epab*$^{-/-}$ oocytes did not undergo GVBD, compared with 74.3 % and 72.5 % of uninjected and injected *Epab*$^{+/+}$ oocytes, respectively. The results are presented as means ± S.E.M; ***P < 0.001. (**B**) At 18 h, *Epab* mRNA-injected and uninjected oocytes were assessed for polar body extrusion (MII stage). Uninjected or injected Epab$^{-/-}$ oocytes did not demonstrate polar body extrusion, compared with 44.3 % and 40.6 % of uninjected and injected *Epab*$^{+/+}$ oocytes respectively. Results are presented as means ± S.E.M.; ***P < 0.001. (**C**) Western blot with an anti-HA antibody was performed in uninjected and injected oocytes (n = 10 per sample) of WT and *Epab*$^{-/-}$ mice to determine EPAB–HA protein expression. Uninjected oocytes did not express the HA-tagged-protein, whereas a protein of the correct size was detected in injected WT and Epab$^{-/-}$ oocytes.

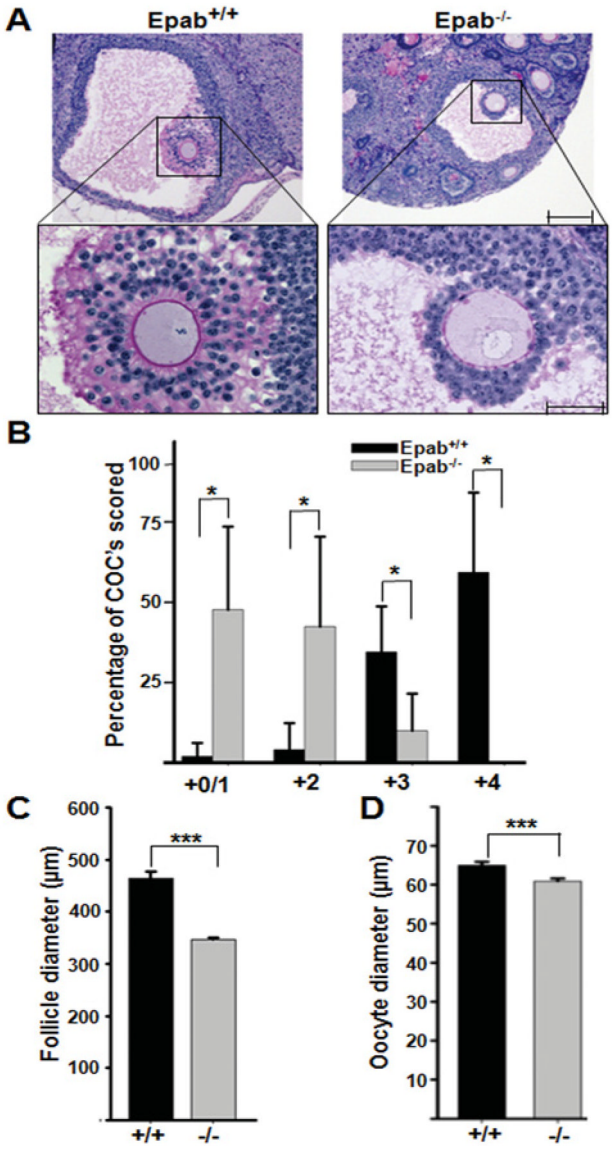

Figure 7. *Epab* is required for normal cumulus expansion

Cumulus expansion was assessed in the ovaries of hyperstimulated 10–12-week-old WT and *Epab*$^{-/-}$ mice ($n = 4$ for each genotype), collected 9 h after the hCG injection. (**A**) Representative micrographs of antral follicles (upper frame) and COCs (insert and lower frame) from WT (*Epab*$^{+/+}$) and *Epab*$^{-/-}$ mice. More compact COCs and a lower number of granulosa cell layers was observed in *Epab*$^{-/-}$ mice. Scale bar represents 50 μm. (**B**) The degree of cumulus expansion was evaluated for COCs in preovulatory follicles of WT (black bars) and *Epab*$^{-/-}$ (grey bars) mice as described previously [31]. The results represent the mean percentage of COCs for each score ± S.E.M.; *$P < 0.05$. (**C**) The diameter of the antral follicles was measured in the ovaries of WT (black bar) and *Epab*$^{-/-}$ (grey bar) mice. The results represent the means ± S.E.M.; ***$P < 0.001$. (**D**) The diameter of the oocytes contained within antral follicles was measured in the ovaries of WT (black bar) and *Epab*$^{-/-}$ (grey bar) mice. The results represent the means ± S.E.M.; ***$P < 0.001$.

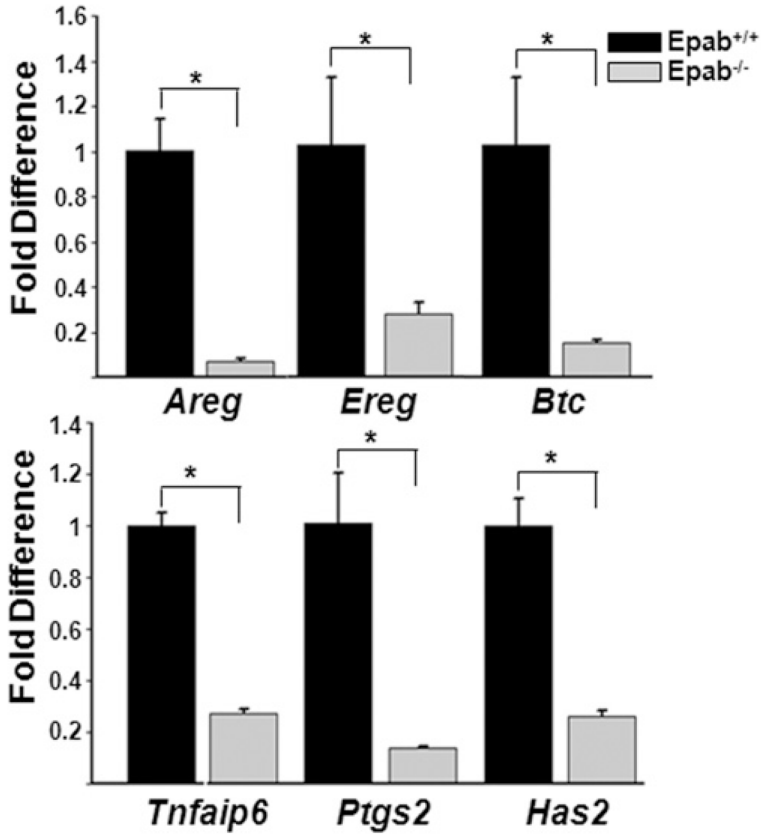

Figure 8. *Epab* is required for the expression of genes that regulate cumulus expansion

Ovaries of superovulated 10–12-week-old WT ($Epab^{+/+}$) or $Epab^{-/-}$ mice ($n = 5$ for each group) were collected 4 h after hCG injection. COCs were obtained by ovarian puncture and cumulus cells were isolated. The expression of *Areg*, *Ereg*, *Btc*, *Ptgs2*, *Has2* and *Tnfaip6* was assessed using qRT-PCR. Expression of the target gene was normalized to β-actin levels. The $2^{-\Delta\Delta C_t}$ (cycle threshold) method was used to calculate relative expression levels. Results were reported as a fold change in gene expression between WT (black bars) and $Epab^{-/-}$ mice (grey bars). The results are presented as means ± S.E.M.; $^*P < 0.05$.

Table 1

***Epab*$^{-/-}$ female mice are infertile**

Fertility of WT (*Epab*$^{+/+}$), *Epab*$^{+/-}$ and *Epab*$^{-/-}$ female mice (*n* = 9 for each genotype) was assessed by mating with WT males of proven fertility (male/female; 1:2) for 20 weeks. There were no pregnancies or deliveries observed in *Epab*$^{-/-}$ female mice, whereas WT and *Epab*$^{+/-}$ females exhibited normal fertility. Results are presented as means ± S.D.;

Genotype	*n*	Litters	Pups	Pups per litter	Litters per female
Epab$^{+/+}$	9	48	385	8.02 ± 2.47	5.33 ± 1.22
Epab$^{+/-}$	9	46	365	7.93 ± 2.14	5.11 ± 0.6
Epab$^{-/-}$	9	0	0	0***	0***

*** $P < 0.001$ for *Epab*$^{-/-}$ compared with *Epab*$^{+/+}$ or *Epab*$^{+/-}$ mice.